ARTICLE

Loss of white matter integrity reflects tau accumulation in Alzheimer disease defined regions

Jeremy F. Strain, PhD, Robert X. Smith, PhD, Helen Beaumont, PhD, Catherine M. Roe, PhD, Brian A. Gordon, PhD, Shruti Mishra, MD, Babatunde Adeyemo, PhD, Jon J. Christensen, PhD, Yi Su, PhD, John C. Morris, MD, Tammie L.S. Benzinger, MD PhD, and Beau M. Ances, MD, PhD

Correspondence
Dr. Ances
bances@wustl.edu

Neurology® 2018;91:e313-e318. doi:10.1212/WNL.0000000000005864

Abstract

Objective

White matter (WM) projections were assessed from Alzheimer disease (AD) gray matter regions associated with β-amyloid (Aβ), tau, or neurodegeneration to ascertain relationship between WM structural integrity with Aβ and/or tau deposition.

Methods

Participants underwent diffusion tensor imaging (DTI), PET Aβ ([^{18}F]AV-45 [florbetapir]), and PET tau ([^{18}F]AV-1451 [flortaucipir]) imaging. Probabilistic WM summary and individual tracts were created from either a composite or individual gray matter seed regions derived from Aβ, tau, and neurodegeneration. Linear regressions were performed for Aβ, age, tau and WM hyperintensities (WMH) to predict mean diffusivity (MD) or fractional anisotropy (FA) from the corresponding WM summaries or tracts.

Results

Our cohort was composed of 59 cognitively normal participants and 10 cognitively impaired individuals. Aβ was not associated with DTI metrics in WM summary or individual tracts. Age and WMH strongly predicted MD and FA in several WM regions, with tau a significant predictor of MD only in the anterior temporal WM.

Conclusion

Tau, not Aβ, was associated with changes in anterior temporal WM integrity. WMH, a proxy for vascular damage, was strongly associated with axonal damage, but tau independently contributed to the model, suggesting an additional degenerative mechanism within tracts projecting from regions vulnerable to AD pathology. WM decline was associated with early tau accumulation, and further decline may reflect tau propagation in more advanced stages of AD.

From the Department of Neurology (J.F.S., R.X.S., H.B., C.M.R., S.M., B.A., J.C.M., B.M.A.), Department of Radiology (B.A.G., J.J.C., Y.S., T.L.S.B., B.M.A.), Knight Alzheimer's Disease Research Center (B.A.G., J.C.M., T.L.S.B., B.M.A.), Department of Pathology (J.C.M.), and Hope Center for Neurological Disorders (J.C.M., B.M.A.), Washington University in St. Louis, MO.

Go to Neurology.org/N for full disclosures. Funding information and disclosures deemed relevant by the authors, if any, are provided at the end of the article.

Glossary

AD = Alzheimer disease; **CDR** = Clinical Dementia Rating; **DTI** = diffusion tensor imaging; **FA** = fractional anisotropy; **FSL** = FMRIB Software Library; **MD** = mean diffusivity; **ROI** = region of interest; **WM** = white matter; **WMH** = white matter hyperintensities; **WUSM** = Washington University in St. Louis School of Medicine.

Alzheimer disease (AD) pathology involves the propagation and accumulation of 2 proteinaceous deposits, β-amyloid (Aβ) plaques and neurofibrillary tangles composed of hyperphosphorylated tau. The posited temporal etiology occurs decades before clinical presentation and involves accumulation of Aβ, followed by increased tau pathology and then neurodegeneration.[1] The pattern of neurodegeneration is spatially distinct and correlates more with tau compared to Aβ. Although a relationship has been observed between tau and atrophy, little is known as to whether tau decreases white matter (WM) integrity.[2] WM damage seen with AD has been attributed largely to vascular changes, but AD pathology exacerbates axonal damage.[3] Loss of WM integrity can result from hyperphosphorylation of tau. This hyperphosphorylation leads to a loss of binding to microtubules, causing reduced structural integrity within the axon.[4]

Prior studies have used amyloid PET,[5] tau PET,[6] and neurodegeneration (structural MRI)[2] to define distinct compilations of gray matter regions that delineate AD stage. Each biomarker contributes to the pathophysiology of AD, and a set of distinct regions can be used to define a particular measure (Aβ, tau, or neurodegeneration). It remains unclear how the presence of Aβ or tau can affect WM projections from AD-signature regions that are spatially distinct from vascular damage. This study focuses on whether Aβ or tau accumulation contributes to degeneration of WM projections from AD-signature regions determined by Aβ, tau, or neurodegeneration.

Methods

Standard protocol approvals, registrations, and patient consents

Participants were recruited by the Charles and Joanne Knight Alzheimer's Disease Research Center at the Washington University in St. Louis School of Medicine (WUSM). Informed consent was obtained from all participants and approved by the WUSM Human Research Protection Office.

Demographics

All participants (n = 70) (46–90 years old) underwent amyloid PET, tau PET, and MRI to derive fractional anisotropy (FA) and mean diffusivity (MD) maps (table 1). Those with symptomatic AD were differentiated from cognitively normal controls with a score of ≥0.5 on the CDR.[7] Biomarker (Aβ) positivity for this cohort was based on previous mean Aβ cortical binding potential (>1.22) derived from a separate group.[5,8] Our cohort was composed of 59 cognitively normal controls (13 amyloid positive) and 10 cognitively impaired individuals (all amyloid positive). All of the cognitively impaired were biomarker positive. No individuals had a CDR score >0 and were not amyloid positive. Vascular risk was scored by summating key demographic variables that associate with vascular risk, including diabetes mellitus, smoking, hyperlipidemia, hypertension, hypercholesterol, atrial fibrillation, angioplasty, congestive heart failure, angina, myocardial infarct, and heart valve (table 1).

MRI acquisition

MRI scans were acquired with a 3T Siemens Biograph mMR scanner (Siemens Medical Solutions, Erlangen, Germany) with a standard 12-channel head coil. A high-resolution structural scan was acquired with a 3-dimensional sagittal T1-weighted magnetization-prepared rapid gradient echo (echo time 16 milliseconds, repetition time 2,400 milliseconds, inversion time 1,000 milliseconds, flip angle 8°, 256 × 256 acquisition matrix, 1 × 1 × 1 mm voxels) using the Alzheimer's Disease Neuroimaging Initiative protocol. One diffusion-weighted scan was also obtained (2.5 × 2.5 × 2.5, repetition time 11,000 milliseconds, echo time 87 milliseconds, flip angle 90°, 64 directions, b value 1,000 s/mm^2) for each participant.

Aβ PET images were simultaneously acquired on the same Biograph mMR scanner (Erlangen, Germany) after a single IV bolus injection of ≈10 mCi of florbetapir ([^{18}F]AV-45). Data from the 50- and 70-minute postinjection window were analyzed.[8] In a separate session, tau PET imaging was acquired on a Biograph40 PET/CT scanner after IV administration of 9 to 13 mCi of flortaucipir ([^{18}F]AV-1451).[9] Data from the 80- to 100-minute postinjection window were analyzed.

Positron emission tomography

Both Aβ and tau tracers were analyzed with a previously described region-of-interest (ROI) pipeline developed at WUSM.[6,10,11] Regional standardized uptake value ratios were obtained with the cerebellar gray matter as a reference region,[14] and partial volume correction was performed with a regional spread function technique.[11,12] Standardized uptake value ratio values were calculated from the segmented T1-weighted images processed with FreeSurfer 5.3 (surfer.nmr.mgh.harvard.edu/) to define cortical and subcortical ROIs.

Gray matter ROI preprocessing

Nine cognitively healthy participants (age 22–35 years) from the Human Connectome Project were selected after rigorous screening of the imaging data (humanconnectome.org/

Table 1 Demographic table

No.	69
Age, mean (SD), y	69.7 (9.05)
M/F, n	29/40
Education, y	15.97 (1.82)
Race (white/black/Asian), n	63/5/1
CDR score > 0	10
Amyloid positive	23
Vascular risk factors, mean (SD), n	1.94 (1.16)

Abbreviation: CDR = Clinical Dementia Rating.

documentation/). The WU-Minn Consortium supplies cortical, subcortical, and tissue segmentations for each participant using FreeSurfer version 5.2.0. Aβ seeds included the prefrontal, gyrus rectus, lateral temporal, and precuneus. Tau seeds included the lateral occipital, inferior temporal, entorhinal, and amygdala. Neurodegenerative seeds included the medial temporal, lateral temporal, inferior temporal, precuneus, inferior parietal, and superior parietal regions. Interface voxels were created by expanding the edges of each cortical/subcortical ROI and multiplied by the corresponding participants WM segmentation mask. From the gray/white segmentations, we identified the corresponding interface voxels for each region that were used as seeds for probabilistic tractography.

WM track preprocessing

Bilateral AD-signature seed regions were evaluated based on a priori topographic knowledge of amyloid PET,[5] tau PET,[6] and neurodegenerative atrophy[2] that differentiated symptomatic AD (CDR score >0) from cognitive normal participants (CDR score 0). Summary PET values were calculated for regions designated as Aβ (A-summary), tau (T-summary), or neurodegeneration (N-summary). WM projections emanating from the interface voxels of each ROI were created by FMRIB Software Library's (FSL's) probabilistic pipeline on the same 9 Human Connectome Project participant described in the previous section.[13] Diffusion data was already preprocessed by the WU-Minn Consortium.[14] This pipeline consisted of correction for EPI distortions, eddy-current–induced distortions, participant motion, and gradient nonlinearities with TOPUP and EDDY from FSL.[15,16]

BedpostX from FSL was used to quantify diffusion parameters on the preprocessed data.[13] This tool uses Markov chain Monte Carlo sampling to calculate the dominant and secondary fiber distributions for each voxel. Each gray matter ROI, in native space, was treated as a seed region for probabilistic tractography.[13] A single exclusion mask was used in the sagittal plane for the EH projections in the T-regions anterior to the body of the hippocampus. The exclusion of these fibers was necessary to diminish the degree of overlap with projections from the amygdala due to their close proximity. On completion, the threshold of each probabilistic mask was 10% of the maximal intensity to reduce sporadic projections. While no optimal threshold has yet been established, this relatively low threshold has previously been deemed appropriate.[16]

All individual probabilistic masks were warped into the Montreal Neurological Institute space with a combination of linear and nonlinear alignments. All probabilistic masks pertaining to a particular track were combined across participant and then limited to voxels present in a majority of participants. One methodologic complication with diffusion tensor imaging (DTI) tractography is that WM voxels may contain information for multiple tracks. To ensure that no voxel was overrepresented, a data-driven algorithm was incorporated.[17] In short, this approach assigns overlapping voxels by comparing track occupancy adjusted for the relative size of both tracts. Implementing this technique forgoes any arbitrary assignment but can yield slightly different projections, depending on the degree of overlap between each of the subset ROIs. After all voxels have been uniquely assigned to 1 track, any voxel that is not contiguous with the main cluster is removed. These tracks served as ROIs with a summary of all WM tracts that project from the A-summary, T-summary, and N-summary regions or individual tracts from each seed region (figure 1).

Calculation of diffusion metrics for the cohort

Preprocessing included correction for motion and eddy-current distortions followed by skull stripping[18] with FSL 5.0.9.[15] Rigorous motion inspection was applied after eddy-current correction. Participants who moved >3.5 mm were removed. Tensor calculation for FA, MD, axial diffusivity, and radial diffusivity were obtained using FMRIB software library (FSL). Each diffusion metric was smoothed with a 2-mm smoothing kernel and registered to the FMRIB58 FA with a combination of linear and nonlinear alignments.

Unlike gray matter segmentation, WM tracts can travel through the same regions; therefore, voxels can contain information for multiple tracts. To ensure that "overlapped" voxels were not overrepresented in the analyses, a data-driven approach was used to assign them to specific tracts.[17] Because of this methodologic complication, the same seed region can generate different WM tracts, depending on the degree and spatial overlap between Aβ, tau, and neurodegenerative regions.

WM hyperintensities

Delineation of WM hyperintensities (WMH) maps was generated with the open-source lesion segmentation tool for SPM (applied-statistics.de/lst.html). Segmented maps were registered to each participant's b0 image with FLIRT from FSL with a 6-parameter model. The maps are then aligned with the same warp matrix created from the FA images to register the lesion maps into common space with

Figure WM projections created with fMRI of the brain software library (FSL) probabilistic tractography

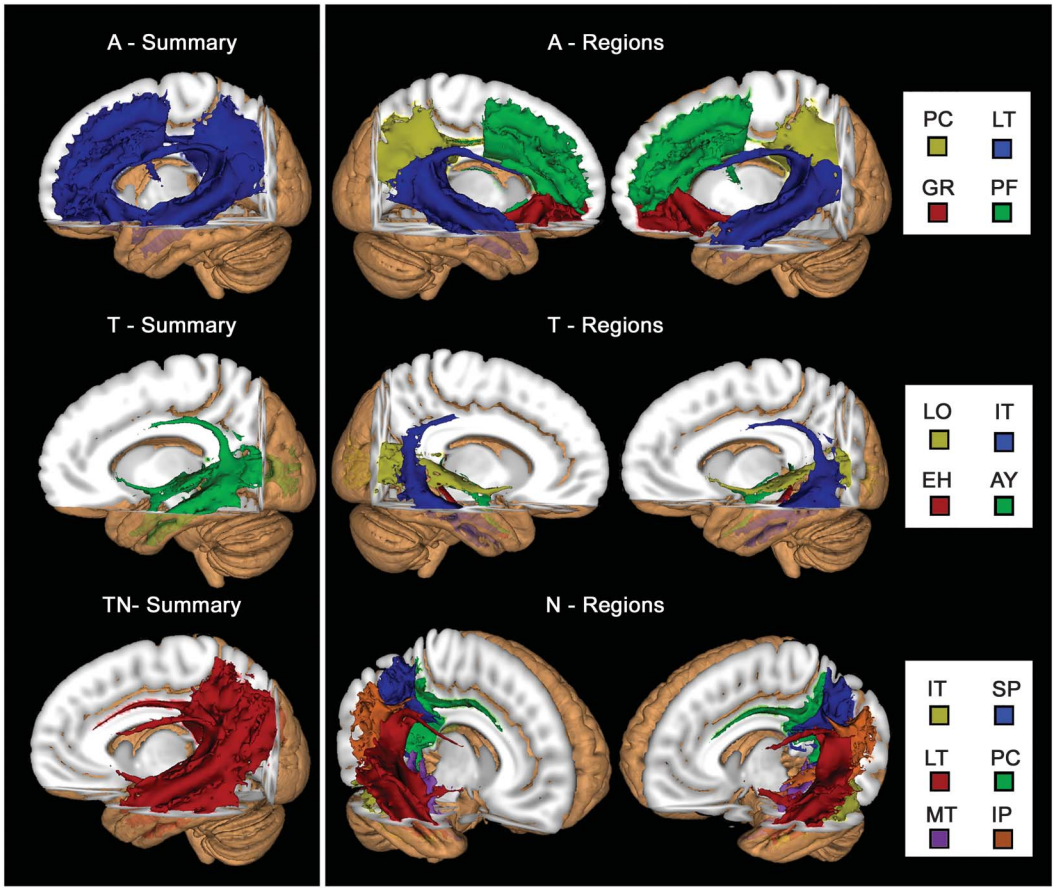

Left, Aggregate white matter (WM) summary of all projections from β-amyloid (A), tau (T), or neurodegenerative (N) regions. Right, Color-coded tracts generated from each set of Alzheimer disease–signature seed regions (A-, T-, N-regions). AY = amygdala; EH = entorhinal; GR = gyrus rectus; IP = inferior parietal; IT = inferior temporal; LO = lateral occipital; LT = lateral temporal; MT = medial temporal; PC = precuneus; PF = prefrontal; SP = superior parietal.

nearest-neighbor interpolation. This allowed us to isolate the lesion voxels that overlapped with our WM tract masks, providing a more localized value of WMH burden. Each voxel that was delineated as lesion, within the tract of interest, was summed to give a total value that was incorporated into the corresponding regression model. We believed this approach was more suitable for our analyses because we were focused on specific WM projections that were created for this study.

Statistics

Linear regression models were performed for WM integrity in each summary tract and included age, amyloid, tau, and WMH as potential predictors. If tau was a significant variable in the summary model, secondary regression models were performed on tracts from each of the regions that made up the summary region. The p values were adjusted for multiple comparisons with false discovery rate.

Data availability

All data are available through the Knight Alzheimer's Disease Research Center (alzheimer.wustl.edu/Research/ResourceRequest.htm).

Results

Demographic information on the entire cohort is found in table 1. One individual who had tau deposition higher than 3 SDs was removed as an outlier and only strengthened the results described below. For projections from the A- and N-summary tracts, only age and WMH predicted WM integrity (all $p < 0.001$). For projections from T-summary tracts, age, WMH, and tau predicted MD. No interactions between any of the variables were significant, and amyloid failed to predict MD or FA in any summary tract. Secondary analyses of regressions for individual T-regions revealed that age and WMH predicted MD for each of the 4 regions. Tau significantly predicted projections from the entorhinal and amygdala (table 2).

Discussion

We focused on 4 variables that relate to WM integrity and AD pathology. No interaction was observed between any of the variables, but rather, independent main effects of age, WMH, and tau best predicted WM integrity in temporal regions.

Table 2 Results of the linear regression for predicting WM integrity

	FA				MD			
	Age	Aβ	Tau	WMH	Age	Aβ	Tau	WMH
Summary results								
A-summary	0.003	0.58	0.86	<0.001	<0.001	0.56	0.94	<0.001
T-summary	0.02	0.74	0.44	<0.001	<0.001	0.58	0.02	<0.001
N-summary	0.01	0.21	0.86	<0.001	<0.001	0.23	0.3	<0.001
T-region summary								
Amygdala	0.002	0.74	0.44	<0.001	<0.001	0.45	0.047	<0.001
Entorhinal	0.07	0.15	0.02	<0.001	0.027	0.55	0.035	<0.001
Inferior temporal	0.13	0.75	0.91	<0.001	<0.001	0.29	0.98	<0.001
Lateral occipital	0.16	0.46	0.57	<0.001	<0.001	0.19	0.08	<0.001

Abbreviations: A = Aβ; Aβ = β-amyloid; FA = fractional anisotropy; MD = mean diffusivity; N = neurodegenerative; T, tau; WM = white matter; WMH = white matter hyperintensities.
Each cell contains the corrected *p* value for each predictive variable.

These results suggest that tau, independently from vascular changes (as assessed by WMH) and Aβ, is a predictor of WM integrity within anterior temporal regions. The main predictors of WM integrity were age and WMH, which are known factors that are associated with myelin breakdown and axonal degeneration. However, the presence of phosphorylated tau is a hallmark of AD, and prior neuroimaging findings showed that tau first accumulates in anterior temporal regions, bolstering the spatial relationship we observed with DTI metrics.[19] We focused on 4 variables that relate to WM integrity and AD pathology. Tau contributed to the model independently of WMH, suggesting that AD pathology can exacerbate axonal damage in addition to vascular changes.

Associations between WM integrity and Aβ have not been consistently found across the literature.[9] In unadjusted analyses, Aβ may serve as a proxy measure for other pathologies (e.g., tau), which are intrinsically associated with it. Aβ pathology was associated with WM integrity when tau and WMH were not included in the regression model (data not shown). However, after tau PET was included in the model, Aβ PET was not associated with any DTI metric. These results suggest that tau is more strongly associated with concurrent neurodegeneration compared to Aβ. The hyperphosphorylation of tau leads to a loss of binding to microtubules, causing loss of structural integrity within the axon.[4] In our data, MD correlated most with tau, implying that this DTI metric is sensitive to early, tau-mediated neurodegeneration.

AD pathology is not uniformly distributed throughout the brain but instead consists of distinct spatial patterns defined by Aβ accumulation, tau accumulation, and structural atrophy.[1] Because of these different spatial profiles, seed regions defined by each biomarker have been previously used to characterize AD progression.[2,5,6] Decline in structural integrity with regard to tau accumulation was strongest in the T-regions, which are more localized to temporal WM changes. Tau propagation is believed to spread via cell-to-cell signaling, causing a neurodegenerative cascade that involves loss of integrity in axonal projections. Tau accumulation is thought to initially occur in the temporal lobe and then propagates to neocortical regions. WM changes may reflect tau propagation out of the temporal lobe to other areas. Future longitudinal studies are needed to ascertain whether DTI metrics could become a clinically relevant biomarker to monitor tau propagation.

The data provided here were driven by the hypothesis that regions susceptible to AD pathology would show WM damage associated with AD biomarkers. The current investigation has limitations. Compared to other studies, our sample size is small. However, as a result of the recent development of tau PET methods, our sample size is one of the largest currently available. Elevated diffusion is associated with cortical atrophy, which is tightly coupled with tau accumulation. However, it is beyond the scope of this project to dissociate WM dysfunction independently of gray matter atrophy.

We show that tau accumulation in anterior temporal regions associates with loss of WM integrity. Age and regional WMH most strongly predicted diffuse WM integrity changes, suggesting that global measurements of structural dysfunction are affected most by non-AD pathology. However, temporal regions are vulnerable to early tau accumulation that is independent of both amyloid and vascular damage. Future studies that include larger populations of individuals with symptomatic AD who are followed up longitudinally are needed. DTI metrics may provide an important biomarker for predicting and monitoring tau progression in symptomatic AD.

Author contributions

J.F.S developed the methodology, conducted the analyses, and prepared the manuscript. C.R assisted in the statistical approaches and preparation of the manuscript. R.X.S., S.M., and B.M.A. assisted in the methodology and reviewing the manuscript. H.B. and B.A.G. assisted in curating the data, overall concept design, and construction of the manuscript. J.J.C. and Y.S. assisted in the PET methodology and assisted in editing the manuscript. J.C.M. contributed to study conception, resources, and project administration. B.M.A. and T.L.S. provided supervision and conception of the study with major contribution to the manuscript.

Acknowledgment

The staff of the Imaging Core at the Knight Alzheimer's Disease Research Center performed imaging acquisition. The authors thank all of the participants for their involvement in this study.

Study funding

This study was funded by NIH grants R01NR012907, R01NR012657, R01NR014449, P50AG05681, P01AG003991, P01AG026276, P30NS048056, UL1TR000448, R01AG04343404, and National Science Foundation grant DMS1300280. Funding was also provided by the Charles F. and Joanne Knight Alzheimer's Research Initiative, the Hope Center for Neurological Disorders, with generous support from the Fred Simmons and Olga Mohan Fund, the Paula and Rodger O. Riney Fund, and the Daniel J Brennan MD Fund. Avid Radiopharmaceuticals (a wholly owned subsidiary of Eli Lilly) provided AV-45 doses and partial financial support for the AV-45 sessions. Avid Radiopharmaceuticals also provided the precursor for AV-1451 and radiopharmaceutical chemistry and technology to the Washington University Investigational New Drug, under which this study was performed.

Disclosure

J. Strain: support for AV-45 and AV-1451 was provided by Avid Radiopharmaceuticals (a wholly owned subsidiary of Eli Lilly). R. Smith, H. Beaumont, and C. Roe report no disclosures relevant to the manuscript. B. Gordon: involved in a clinical trial on AV-1451 sponsored by Avid. S. Mishra, B. Adeyemo, J. Christensen, and Y. Su report no disclosures relevant to the manuscript. J. Morris: currently participating in clinical trials of antidementia drugs developed by Eli Lilly and Co, Biogen, and Janssen. Dr. Morris serves as a consultant for Lilly USA. He receives research support from Eli Lilly/Avid Radiopharmaceuticals. T. Benzinger: involved in a clinical trial that uses AV-1451 sponsored by Avid. B. Ances: involved in a clinical trial that uses AV-1451 sponsored by Avid. Go to Neurology.org/N for full disclosures.

Received January 17, 2018. Accepted in final form April 18, 2018.

References

1. Jack CR Jr, Knopman DS, Jagust WJ, et al. Tracking pathophysiological processes in Alzheimer's disease: an updated hypothetical model of dynamic biomarkers. Lancet Neurol 2013;12:207–216.
2. Wang L, Benzinger TL, Su Y, et al. Evaluation of tau imaging in staging Alzheimer disease and revealing interactions between B-amyloid and tauopathy. JAMA Neurol 2016;73:1070–1077.
3. McAleese KE, Walker L, Graham S, Moya ELJ, Johnson M, et al. Parietal white matter lesions in Alzheimer's disease are associated with cortical neurodegenerative pathology, but not with small vessel disease. Acta Neuropathol 2017;134:459–473.
4. Sexton CE, Kalu UG, Filippini N, et al. A meta-analysis of diffusion tensor imaging in mild cognitive impairment and Alzheimer's disease. Neurobiol Aging 2011;32: 2322.e5–2322.e18.
5. Mintun MA, Larossa GN, Sheline YI, et al. [11C] PIB in a nondemented population: potential antecedent marker of Alzheimer disease. Neurology 2006;67:446–452.
6. Mishra S, Gordon BA, Su Y, et al. Classifying tau PET positivity with [18F]-AV-1451 in preclinical Alzheimer's disease. Alzheimers Demen 2016;12:S2–S3.
7. Morris JC. The Clinical Dementia Rating (CDR): current version and scoring rules. Neurology 1993;43:2412–2414.
8. Su Y, D'Angelo GM, Vlassenko AG, et al. Quantitative analysis of PiB-PET with FreeSurfer ROIs. PLoS One 2013;6:e73377.
9. Brier MR, Gordon B, Friedrichsen K, et al. Tau and Aβ imaging, CSF measures, and cognition in Alzheimer's disease. Sci Transl Med 2016;8:338ra66.
10. Hampel H, Burger K, Teipel SJ, et al. Core candidate neurochemical and imaging biomarkers of Alzheimer's disease. Alzheimers Dement 2008;4:38–48.
11. Su Y, Blazey TM, Synder AZ, et al. Partial volume correction in quantitative amyloid imaging. Neuroimage 2015;107:55–64.
12. Rousset OG, Ma Y, Evans AC. Correction for partial volume effects in PET: principle and validation. J Nucl Med 1998;39:904–911.
13. Behrens TEJ, Johansen-Berg H, Jbabdi S, et al. Probabilistic diffusion tractography with multiple fibre orientations: what can we gain? NeuroImage 2007;34:144–155.
14. Glasser MF, Sotiropoulos SN, Wilson AJ, et al. The minimal preprocessing pipelines for the Human Connectome Project. Neuroimage 2013;80:105–124.
15. Smith SM, Jenkinson M, Woolrich MW, et al. Advances in functional and structural MR image analysis and implementation as FSL. Neuroimage 2004;23:208–219.
16. De Witte NAJ, Mueller SC. White matter integrity in brain networks relevant to anxiety and depression: evidence from the Human Connectome Project dataset. Brain Imaging Behav 2016;11:1604–1615.
17. Strain JF, Didehbani N, Spence J, et al. White matter changes and confrontation naming in retired aging NFL athletes. J Neurotrauma 2016;34:372–379.
18. Smith SM. Fast robust automated brain extraction. Hum Brain Mapp 2002;17: 143–155.
19. Teipel S, Grothe MJ, Zhou, et al. Measuring cortical connectivity in Alzheimer's disease as a brain neural network pathology: toward clinical applications. JINS 2016; 22:138–163.